International Journal of Heat and Technology
Vol. 43, No. 6, December, 2025, pp. 2055-2068
Journal homepage: http://iieta.org/journals/ijht

Thermal Stability Prediction and Structural Optimization of Intelligent Packaging for Light Industry Based on Thermal Network Modeling and Electronic Cooling Simulation

Weixing Xu*, Meng Gao

School of Energy and Intelligence Engineering, Henan University of Animal Husbandry and Economy, Zhengzhou 450011, China

Corresponding Author Email: 80686@hnuahe.edu.cn

https://doi.org/10.18280/ijht.430606

Received: 8 May 2025
Revised: 20 September 2025
Accepted: 12 October 2025
Available online: 31 December 2025

Keywords:
intelligent packaging, thermal network modeling, electronic cooling simulation, thermal stability, multi-objective optimization, cold chain fresh food packaging, sustainable design, digital twin

ABSTRACT

The commercialization of intelligent packaging is increasingly widespread in high-value sectors such as cold chain fresh food and injectable pharmaceuticals. Among these, the thermal stability of cold chain fresh food smart tags is a particularly prominent issue. The continuous heat generated by embedded RFID chips and temperature and humidity sensors can lead to risks such as battery leakage, contamination, disruption of traceability links, and spoilage of fresh products. These risks have become a core bottleneck in scaling the application of intelligent packaging for high-value light industry products. Existing research has limitations such as inadequate scenario specificity, weak physical connotations in thermal network models, and a disconnect between optimization schemes and engineering implementation. This study aims to address the thermal stability issues in cold chain fresh food intelligent packaging by constructing a high-precision, multi-field coupled thermal network model, and establishing a simulation-optimization-experiment closed-loop system. A general structural optimization methodology is proposed that integrates thermal reliability, lightweight design, and sustainability. The research completes the thermal network modeling by node physical equivalence division, nonlinear thermal resistance and capacitance parameter characterization, and the derivation of classic heat transfer differential equations. CFD-FEA coupled simulations and fresh product storage and transportation condition calibration are used to conduct multi-physics electronic cooling analysis. The response surface method is coupled with an improved genetic algorithm for optimization, and advantages over NSGA-II and other algorithms are compared. Parameter sensitivity analysis is conducted using dimensionless numbers such as the Biot number and Fourier number. Finally, experimental validation confirms the effectiveness of the proposed methodology. The experimental results show that the four-node thermal network model has reliable accuracy, with an average absolute error of 0.7℃ and a root mean square error of 1.0℃. The improved genetic algorithm converges 15.6% faster than NSGA-II and produces a more evenly distributed Pareto optimal solution. After optimization, the maximum temperature of the cold chain fresh food packaging is reduced by 18.3%, mass is reduced by 16.2%, and costs are reduced by 11.5%, with the fresh product storage and transportation loss rate dropping to 3.3%. The experimental and simulation errors are ≤3.8%, and the methodology, when applied to flexible electronics, can achieve a 17.6% improvement in thermal stability. This study brings innovation in three dimensions: multi-field coupled thermal network physical equivalence modeling, interdisciplinary closed-loop optimization framework, and transferable methodology for customized scene solutions. It provides academic support for the interdisciplinary fields of packaging engineering, heat transfer science, and electronic engineering, and contributes to the advancement of the green intelligent packaging industry.

1. INTRODUCTION

The deep integration of intelligent packaging technology with the light industry has accelerated its commercialization in high-value fields such as cold chain fresh food, injectable pharmaceuticals, and high-end cosmetics [1-3]. These types of packaging, by integrating functions such as sensing and communication modules, play an irreplaceable role in key processes like product traceability, quality monitoring, and anti-counterfeiting verification, significantly enhancing the added value and market competitiveness of light industry products. Among them, cold chain fresh food smart tags, as typical representatives, need to operate for long periods in dynamic storage and transportation environments ranging from -10 to 25℃ [4, 5]. The temperature fluctuations in the environment and the continuous heat generated by embedded electronic components create a complex thermal coupling, making their thermal management needs one of the industry's

most urgent technical challenges. The issue of thermal runaway directly triggers multiple industrial risks—continuous heat from embedded RFID chips and temperature and humidity sensors can lead to battery leakage, contamination of fresh food [6, 7], high temperatures can cause chip thermal failure and break the traceability link [8], and localized temperature exceeding the cold chain threshold accelerates the spoilage and deterioration of fresh products [9]. According to industry reports, such thermal-related problems result in global cold chain fresh food industry losses exceeding 100 billion USD annually. Therefore, solving the thermal stability problem of cold chain fresh food intelligent packaging is crucial for ensuring product safety and reducing industry losses. This research is based on the cross-integration of packaging engineering, heat transfer science, electronic engineering, and optimization algorithms, aiming to address the thermal management challenges of specific scenarios by constructing a universal methodology framework. This framework can not only be directly applied to the design optimization of cold chain fresh food intelligent packaging but also provide technical references for thermal management research in flexible electronics, wearable devices, and other fields, helping the intelligent packaging industry upgrade toward green sustainability, with both significant academic and engineering application value.

Research in the field of intelligent packaging thermal analysis has made certain progress, but existing results exhibit clear limitations in specific scenarios. Most studies focus on normal-temperature static conditions, and there is a lack of specialized research on dynamic fluctuating conditions like cold chain fresh food. Moreover, existing thermal analysis models generally ignore the multi-medium thermal coupling effects between packaging, content, and environment [10], making it difficult to accurately characterize the heat transfer laws in actual storage and transportation processes. Thermal network modeling technology, because it balances computational efficiency and engineering accuracy, has been widely used in thermal analysis in fields such as electronic devices and power batteries [11, 12]. However, its application in light industry intelligent packaging remains significantly insufficient. Most related models directly apply node division schemes from other fields [13], lacking a physical equivalence demonstration for the packaging-content coupling system. Node division often fails to balance engineering accuracy and computational efficiency, leading to a gap between model prediction accuracy and actual application requirements. Multi-physics field simulation technology is becoming more mature in the field of electronic cooling [14, 15], but its lack of synergy with optimization algorithms restricts its deep application in the light industry packaging field. In existing research, the selection of optimization algorithms often lacks systematic comparative analysis, and the optimization targets are primarily focused on thermal performance improvement [16, 17], without fully addressing the core engineering needs of lightweight design, low cost, and ease of production for light industry packaging, thereby significantly reducing the engineering applicability of optimization schemes. It is also noteworthy that sustainable design concepts have not been sufficiently emphasized in intelligent packaging thermal management research. Most existing optimization schemes focus on balancing thermal performance and cost [18-20], without establishing the link between lightweight design and green packaging, resource conservation, resulting in a disconnect between the industrial and social value of research results and limiting their potential for engineering transformation.

Based on the progress of existing research, there are three major core research gaps in the field: (1) In the scenario and theoretical aspect, there is a lack of dedicated thermal network models for cold chain fresh food dynamic conditions. Existing models have not explained the physical equivalence relationship between discrete nodes and continuous heat transfer media, leading to insufficient thermal stability prediction accuracy. (2) In the method and algorithm aspect, the synergy mechanism between thermal simulation and multi-objective optimization is incomplete. The selection of algorithms lacks targeted comparative analysis, and the "modeling-simulation-optimization-validation" closed-loop research system has not been established, limiting the research efficiency and reliability. (3) In the application and value aspect, optimization schemes generally overlook the balance between engineering feasibility and sustainability, and no universal methodology framework has been constructed to facilitate cross-field transfer, leading to a disconnect between research results and industrial practical needs, making it difficult to support the implementation of technology in multiple scenarios.

To address the above research gaps, this study focuses on solving the thermal stability problem of cold chain fresh food intelligent packaging, setting three major research goals: (1) to establish a multi-field coupled thermal network model with physical equivalence for accurate thermal stability prediction, (2) to construct a universal methodology framework for "thermal network modeling-multi-physics field simulation-multi-objective optimization-experimental validation," and (3) to propose a structural optimization scheme that balances thermal reliability, lightweight design, and green sustainability, and verify its cross-field transferability. The core research contents of this study include four aspects: (1) Conducting an analysis of the heat transfer mechanism of cold chain fresh food intelligent packaging, completing the physical equivalence construction of the thermal network model, and clarifying the characterization method for thermal resistance and thermal capacitance parameters under multi-medium coupling; (2) Establishing a multi-physics field coupled electronic cooling simulation model, calibrating boundary conditions based on cold chain fresh food storage and transportation dynamic conditions, ensuring the consistency of simulation results with actual conditions; (3) Using the response surface method and improved genetic algorithm for coupling optimization, systematically comparing the optimization performance of algorithms such as NSGA-II and MOEA/D, and determining the optimal algorithm combination for this study; (4) Conducting experimental verification of the optimization scheme, completing an engineering feasibility analysis, and testing its transferability in the flexible electronics field to verify the universality of the methodology framework.

The innovations of this study are mainly reflected in three dimensions: (1) Theoretical innovation: The "component-packaging-fresh food-environment" four-level node thermal network model is proposed, addressing the physical equivalence relationship between discrete nodes and continuous heat transfer media, compensating for the lack of physical connotation in existing models. The introduction of nonlinear thermal resistance parameters improves thermal stability prediction accuracy under dynamic conditions. (2) Methodological innovation: The interdisciplinary closed-loop

optimization framework is constructed, systematically demonstrating the coupling advantages of the response surface method and the improved genetic algorithm, solving the problem of insufficient synergy between thermal simulation and optimization algorithms. The use of dimensionless analysis tools such as the Biot number and Fourier number realizes the universal characterization of parameter sensitivity, enhancing the general value of research results. (3) Application innovation: A customized structural optimization scheme for cold chain fresh food scenarios is proposed, achieving precise balancing of thermal performance, lightweight design, and cost. A universal methodology transfer mechanism is established, verifying its applicability in flexible electronics and other fields through cross-field testing, and deeply binding lightweight design with green sustainability concepts, improving the industrial value of the research.

This paper follows the logical thread of "problem identification-theoretical modeling-simulation optimization-experimental verification-methodology transfer-value enhancement". The following chapters will systematically explain the theoretical foundation and related technologies required for the research, detail the research methods and experimental design, clarify the parameters of the research objects, the process of thermal network model construction, simulation model calibration methods, optimization scheme design, and experimental verification system. The key results of thermal network model verification, thermal stability prediction, structural optimization, and cross-field transfer testing will be presented and analyzed. The physical mechanisms behind the core results, the differences with existing research, engineering transformation value, research limitations, and future research directions will be deeply discussed. Finally, the study's conclusions will be summarized, highlighting core innovations and academic contributions, and forecasting the engineering application prospects.

2. RESEARCH METHODS AND EXPERIMENTAL DESIGN

2.1 Definition of research objects: Cold chain fresh food intelligent packaging prototype

This research focuses on the thermal stability prediction and structural optimization of cold chain fresh food intelligent packaging. The research object is defined as the "electronic components - three-layer composite packaging - fresh products" coupling system. The design of each part is centered around the electronic cooling demand and thermal stability improvement goals of "suppressing heat accumulation and enhancing heat dissipation." The packaging adopts a three-layer composite structure of "outer heat-insulating membrane - middle buffer layer - inner freshness-preserving layer," with material selection focusing on the correlation between thermal physical properties and thermal stability: The outer heat-insulating membrane uses high-density polyethylene (HDPE), with thermal conductivity $\lambda_1 = 0.42$ W/(m·K), specific heat capacity $c_{p1} = 2300$ J/(kg·K), and density $\rho_1 = 950$ kg/m^3. Its main function is to block external thermal disturbances and reduce heat flow intrusion. The middle buffer layer uses expanded polystyrene (EPS), with thermal conductivity $\lambda_2 = 0.038$ W/(m·K), specific heat capacity $c_{p2} = 1300$ J/(kg·K), and density $\rho_2 = 25$ kg/m^3, constructing an internal thermal resistance barrier through high insulation properties, suppressing heat transfer from the electronic components to the fresh food area. The inner freshness-preserving layer uses polyvinyl chloride (PVC), with thermal conductivity $\lambda_3 = 0.16$ W/(m·K), specific heat capacity $c_{p3} = 1900$ J/(kg·K), and density $\rho_3 = 1380$ kg/m^3, balancing air tightness and low-temperature adaptability to prevent local thermal convection caused by internal airflow disturbances. The packaging dimensions are 150 mm × 100 mm × 50 mm, with initial thicknesses of 0.15 mm for the outer layer, 15 mm for the middle layer, and 0.1 mm for the inner layer. This design is suitable for small fresh food packaging scenarios and leaves room for optimization in the thickness range.

The embedded electronic components serve as the core heat source, and their selection and arrangement directly affect thermal stability: The RFID chip used is the Impinj Monza R6, with dimensions of 1.6 mm × 1.6 mm × 0.18 mm and a rated heat dissipation power Q_1 = 0.12 W; the temperature and humidity sensor used is the SHT30, with dimensions of 2.5 mm × 2.5 mm × 0.9 mm and a rated heat dissipation power Q_2 = 0.08 W, with measurement accuracy of ±0.3°C and ±2% RH, providing baseline data for thermal stability verification. Both components are fixed to the surface of the fresh food using flexible adhesive, with a spacing of 15–30 mm and a distance of 20 mm from the packaging edge. This arrangement avoids interference from temperature gradients at the edges, ensuring uniform heat source distribution while minimizing the occupation of fresh food placement space.

The cold chain storage and transportation conditions are based on full-link measured data, simulating real thermal disturbance environments to ensure the engineering applicability of the research: The temperature range is −10 to 25°C, covering refrigerated storage (0–4°C), low-temperature transportation (−10 to 0°C), and room temperature transfer (15–25°C), with convective speed ranging from 0.5 to 2 m/s and relative humidity ranging from 60% to 90% RH. The condition parameters fluctuate dynamically in a 4-hour cycle, with temperature and convective speed time-series curves fitted from industry-measured data, providing boundary conditions that closely match actual conditions for dynamic thermal stability prediction.

2.2 Thermal network model construction and verification

2.2.1 Node system and thermal physical parameter determination

This study is based on the "heat generation - heat transfer - heat dissipation" full thermal transfer path and follows the principle of physical equivalence to establish the four-level node system of "electronic components - packaging functional layer - fresh products - environment." The core goal is to accurately characterize the thermal transfer law of the coupling system and achieve dynamic thermal stability prediction. In terms of node definitions and parameters, the electronic component node integrates the RFID chip and temperature and humidity sensor, which are treated as a concentrated heat source with total heat dissipation power $Q = Q_1 + Q_2 = 0.2$ W. The thermal capacitance $C_1 = m_1c_{p1} + m_2c_{p2}$, where m_1 and m_2 are the masses of the two components. The packaging functional layer node is divided according to the three-layer structure: outer heat-insulating membrane, middle buffer layer, and inner freshness-preserving layer. The thermal resistance for each layer is $R_i = \delta_i/(\lambda_i A)$, where δ_i is the thickness and A is the heat transfer area; the thermal

capacitance is $C_i = \rho_i V_i c_{pi}$, where V_i is the volume. The fresh product node uses the equivalent volume method to integrate the heterogeneous fresh food. The equivalent thermal resistance R_{fresh} is measured using the steady-state plate method: A constant temperature hot plate-cold plate experimental device is used to measure the steady-state heat flux density q and the temperature difference ΔT between the upper and lower surfaces of the fresh food. Based on Fourier's law, the equivalent thermal conductivity λ_{fresh} is calculated:

$$q=\lambda_{fresh}\Delta T/\delta_{fresh} \tag{1}$$

Then, calculate:

$$\bar{R}_{fresh}=\delta_{fresh}/(\lambda_{fresh}A) \tag{2}$$

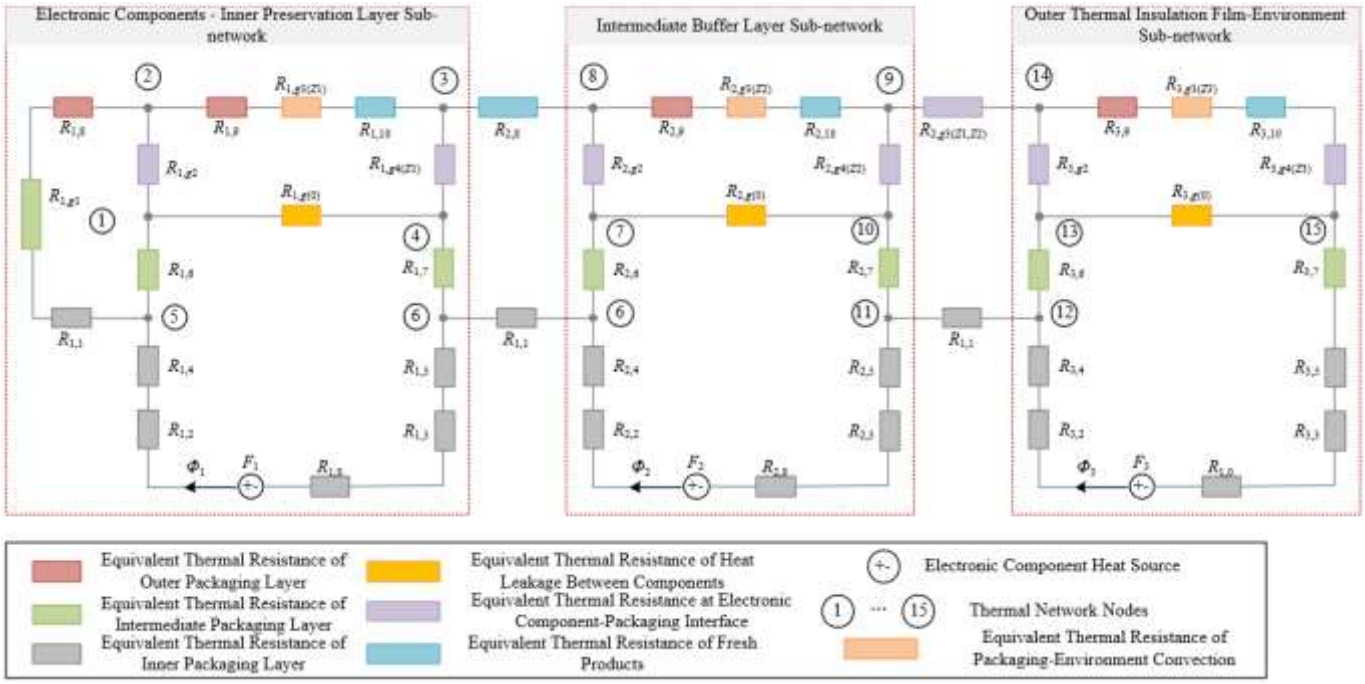

Figure 1. The four-level node equivalent thermal network model of cold chain fresh food intelligent packaging

The environment node represents the dynamic working conditions, and the convective heat transfer coefficient h is calculated based on the Nusselt number correlation formula, providing boundary conditions for the subsequent thermal balance equations.

Figure 1, using cold chain fresh food intelligent packaging as an example, shows the four-level node equivalent thermal network model of "electronic components - packaging functional layer - fresh products - environment," clearly presenting the thermal resistance relationships and heat transfer paths between the nodes, intuitively demonstrating the physical equivalence between discrete nodes and continuous heat transfer media.

2.2.2 Mathematical derivation of the thermal network model

Based on the thermal balance principle and Kirchhoff's current law, the nonlinear thermal balance equations for each node are derived. Using the core electronic component node and the middle buffer layer node as examples, the complete derivation process is as follows:

The heat flow into the electronic component node is its own heat generation power Q, and the heat flow out is the conductive heat flow to the inner freshness-preserving layer $(T_1-T_4)/R_{14}$. The thermal balance equation is:

$$C_1\frac{dT_1}{dt}=Q-\frac{T_1-T_4}{R_{14}} \tag{3}$$

The heat flow into the middle buffer layer node is the conductive heat flow from the outer heat-insulating membrane $(T_2-T_3)/R_{23}$, and the heat flow out is the conductive heat flow to the inner freshness-preserving layer $(T_3-T_4)/R_{34}$. The thermal balance equation is:

$$C_3\frac{dT_3}{dt}=\frac{T_2-T_3}{R_{23}}-\frac{T_3-T_4}{R_{34}} \tag{4}$$

The heat flow into the fresh product node is the conductive heat flow from the inner freshness-preserving layer $(T_4-T_5)/R_{45}$, and the heat flow out is the convective heat flow to the environment $hA(T_5-T_{env})$. The thermal balance equation is:

$$C_5\frac{dT_5}{dt}=\frac{T_4-T_5}{R_{45}}-hA(T_5-T_{env}) \tag{5}$$

Integrating the four-level nodes, we get the system's overall nonlinear differential equation set:

$$\begin{cases} C_1\dfrac{dT_1}{dt}=Q-\dfrac{T_1-T_4}{R_{14}} \\ C_2\dfrac{dT_2}{dt}=hA(T_{env}-T_2)-\dfrac{T_2-T_3}{R_{23}} \\ C_3\dfrac{dT_3}{dt}=\dfrac{T_2-T_3}{R_{23}}+\dfrac{T_3-T_4}{R_{34}} \\ C_4\dfrac{dT_4}{dt}=\dfrac{T_1-T_4}{R_{14}}+\dfrac{T_3-T_4}{R_{34}}-\dfrac{T_4-T_5}{R_{45}} \\ C_5\dfrac{dT_5}{dt}=\dfrac{T_4-T_5}{R_{45}}-hA(T_5-T_{env}) \end{cases} \tag{6}$$

where, the nonlinearity arises from the dynamic changes in the

convective heat transfer coefficient h and thermal resistance R_{ij} with temperature. The finite difference method is used to discretize the equation set, with a time step of Δt = 0.1 s. A MATLAB program is written to solve the equations, and the temperature-time curves for each node are output. The core prediction indicator is the maximum temperature of the electronic component T_{max}.

2.2.3 Model verification experimental design

Infrared temperature measurement experiments are used to verify the prediction accuracy of the thermal network model. The experimental platform consists of a constant temperature and humidity chamber, a high-precision infrared thermal imager, and a data acquisition system. Key measurement nodes are selected on the surface of the electronic components, the inner layer of the packaging, the center of the fresh product, and the outer surface of the packaging. Under the set dynamic cold chain conditions, temperature data from the experiments and model predictions are collected synchronously, with the sampling interval consistent with the model calculation step length. The model accuracy is quantified by calculating the mean absolute error (MAE) and root mean square error (RMSE). The error calculation formulas are as follows:

$$MAE=\frac{1}{N}\sum_{k=1}^{N}|T_{pred,k}-T_{exp,k}|, \tag{7}$$

$$RMSE=\sqrt{\frac{1}{N}\sum_{k=1}^{N}(T_{pred,k}-T_{exp,k})^2} \tag{8}$$

where, $T_{pred,k}$ is the model predicted temperature, $T_{exp,k}$ is the experimental measured temperature, and N is the number of sampling points. When MAE is less than 1℃ and RMSE is less than 1.5℃, the model prediction accuracy is considered to meet engineering requirements, ensuring that the model can be used for subsequent thermal stability analysis and structural optimization.

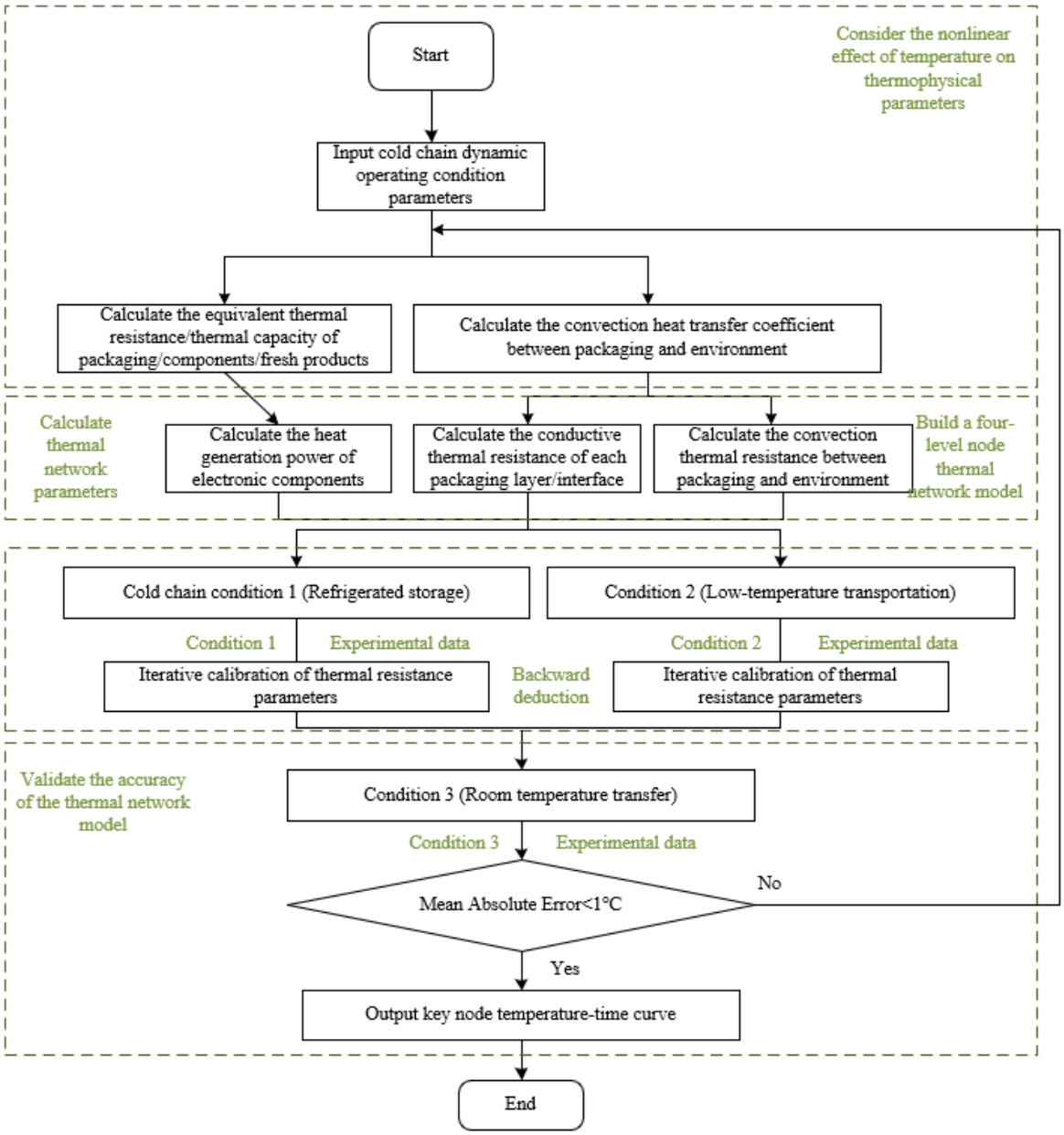

Figure 2. "Simulation-experiment" closed-loop verification process diagram of the cold chain fresh food intelligent packaging thermal network model

Figure 2 shows the "simulation-experiment" closed-loop verification process of the cold chain fresh food intelligent packaging thermal network model. It covers the cold chain dynamic working conditions input, thermal physical parameter calculation, thermal network construction, multi-condition parameter calibration, and MAE/RMSE accuracy determination, fully presenting the closed-loop logic of the model from construction to verification.

2.3 Multiphysics coupled simulation model establishment and calibration

The “electronic components - packaging - fresh food” full-scale coupled geometric model is constructed using ANSYS ICEM. The modeling process strictly follows the actual structural dimensions and assembly relationships of the research object, fully preserving the geometric features of the three-layer packaging structure, electronic components, and fresh products, ensuring the geometric fidelity of the model. Mesh generation uses a hybrid strategy combining unstructured tetrahedral meshes and structured hexahedral meshes. The mesh around the electronic component surface and surrounding areas is refined—this area is treated as the core heat source and the region with significant temperature gradient changes. The mesh size is refined to 0.1 mm to capture local heat transfer details accurately. The packaging body and fresh product areas use relatively coarse meshes to balance computational accuracy and efficiency. To eliminate the impact of mesh density on the simulation results, mesh independence verification is performed: five sets of different mesh densities are sequentially set, and the steady-state temperature on the surface of the electronic components is calculated under the same boundary conditions. When the number of elements reaches 1.5 million, the temperature calculation variation is less than 1%, which is determined to be the optimal mesh solution.

The thermal physical parameters of each medium determined in Section 2.1 are precisely input into the simulation model to achieve accurate material property representation. The boundary conditions are set to equivalently convert the cold chain dynamic working conditions: the outer surface of the packaging uses a convective heat transfer boundary, and the convective heat transfer coefficient at different convective speeds is calculated based on the Nusselt number correlation formula. The boundary conditions are loaded sequentially according to the dynamic temperature curve. The electronic components are treated as volumetric heat source boundaries, and the heat source strength is set according to their rated power to simulate sustained heating characteristics. The specific formula is as follows:

$$Nu=CRe^{m}Pr^{n} \tag{9}$$

Interface thermal resistance boundaries are set on all contact surfaces inside the packaging, with initial values based on literature data. Contact thermal resistance between the fresh product and the inner layer of the packaging and between the packaging layers is set according to the actual assembly state to ensure the accurate representation of the multi-physics coupled heat transfer process.

ANSYS Fluent is used to solve the coupled flow field-temperature field equations, and numerical solutions are based on the finite volume method. The control equations include the continuity equation, momentum equation, and energy equation. For the mixed conditions of natural convection and forced convection in cold chain storage and transportation, the standard k-ε turbulence model is used to close the control equations. The pressure-velocity coupling uses the SIMPLE algorithm, and the energy equation discretization scheme uses a second-order upwind scheme to improve computational accuracy. The simulation is solved in two steps: first, a steady-state simulation is conducted to obtain the baseline temperature distribution, and then a transient simulation is performed to capture the temperature response characteristics under dynamic working conditions. Based on the key node temperature data obtained from the infrared temperature measurement experiments in Section 2.2, interface thermal resistance parameters are iteratively calibrated. The experimental temperatures at the surface of the electronic components, the center of the fresh food, and the outer surface of the packaging are used as target values. The interface thermal resistance values are gradually adjusted until the deviation between the simulation predicted temperatures and the experimental measured temperatures is less than 5%, completing the model calibration and ensuring that the simulation model accurately reflects the actual heat transfer laws.

2.4 Multidimensional structural optimization design

The selection of optimization variables is based on the core structural parameters that affect the thermal stability, lightweight design, and process feasibility of cold chain fresh food intelligent packaging, with the final determination of three key optimization variables. The thicknesses of the packaging layers, including the outer thermal barrier film, the intermediate buffer layer, and the inner preservation layer, are in the ranges of 0.1–0.2 mm, 12–18 mm, and 0.08–0.12 mm, respectively, balancing thermal insulation performance and structural lightweight requirements. The cooling hole parameters, including hole diameter and number, are selected with hole diameters ranging from 2 to 5 mm and the number of holes ranging from 4 to 12, to balance the enhancement of convective heat transfer and packaging structural strength. The arrangement spacing of the electronic components, i.e., the center distance between the RFID chip and the temperature and humidity sensor, ranges from 15 to 30 mm to avoid localized high-temperature accumulation caused by concentrated heat generation. The range of all variables is determined based on the limits of current packaging production processes and preliminary pre-simulation results to ensure the engineering feasibility of the optimization scheme.

The objective functions are set to three mutually conflicting core indicators, with precise mathematical expressions constructed and engineering constraints added to achieve the collaborative optimization of thermal stability, lightweight design, and economic efficiency:

Objective 1 — Maximization of Thermal Stability: Minimize the maximum temperature of the electronic components, $f_1 = min(T_{max})$, with the constraint $Tmax \leq 35$℃;

Objective 2 — Maximization of Lightweight Design: Minimize the total mass of the packaging, $f_2 = min(m)$, where $m = \rho_1 x_1 A+\rho_2 x_2 A+\rho_3 x_3 A$, with A being the packaging surface area;

Objective 3 — Maximization of Economic Efficiency: Minimize the manufacturing cost, $f_3 = min(C)$, where $C = c_1 x_1 A + c_2 x_2 A + c_3 x_3 A + c_4 x_5$, with c_1~c_3 being the material unit prices,

and c_4 being the per-hole processing cost.

2.4.1 Surrogate model construction and optimization solution

A surrogate model of the optimization variables and objective functions is constructed using the response surface methodology, with the Box-Behnken design plan for experiment design. This design does not require touching the boundary values of the variables and can effectively reduce the number of experiments while ensuring the model fitting accuracy. The experimental scheme consists of 27 test points, covering typical combinations of variable values within their ranges, and solving the corresponding objective function values for each test point using the calibrated multiphysics coupled simulation model.

The surrogate model is built based on experimental data to construct a second-order polynomial regression model for the objectives f_1, f_2, and f_3:

$$y=\beta_0+\sum_{i=1}^{6}\beta_i x_i+\sum_{i=1}^{6}\beta_{ii}x_i^{\ 2}+\sum_{1\le i<j\le 6}\beta_{ij}x_i x_j \tag{10}$$

where, y is the objective function, β_0, β_i, β_{ii}, and β_{ij} are the constant, linear, quadratic, and interaction coefficients, respectively. An analysis of variance is conducted to verify the model significance, and the coefficient of determination R^2 and the adjusted coefficient of determination R^2_{adj} are used to evaluate the goodness of fit of the model. The values of R^2 and R^2_{adj} must both exceed 0.95 to ensure the model can accurately represent the mapping relationship between the variables and the objective functions.

An improved genetic algorithm is used to solve the multi-objective optimization problem. The algorithm introduces an elitism strategy and an adaptive crossover-mutation probability mechanism based on traditional genetic algorithms to improve convergence speed and the quality of the optimal solution. The algorithm parameters are set as follows: population size of 100, 50 iterations, initial crossover probability of 0.8, mutation probability of 0.1, with the crossover probability linearly decreasing to 0.6 and the mutation probability linearly increasing to 0.2 during the iteration process, balancing global search and local optimization abilities. The response surface surrogate model is used as the fitness function calculation module to solve the Pareto optimal front in the "temperature-mass-cost" three-dimensional objective space. To verify the superiority of the algorithm, the NSGA-II algorithm is also used for optimization, and a comparison is made in terms of convergence speed and Pareto solution distribution uniformity. Convergence speed is measured by the number of iterations required to reach a stable solution, and the uniformity of the solutions is quantified using the Spacing metric to ensure the optimization performance advantage of the selected algorithm.

The Biot number and Fourier number are introduced to perform dimensionless parameter sensitivity analysis to quantify the influence weight of each optimization variable on thermal stability. The Biot number is defined as:

$$Bi=\frac{hL}{\lambda} \tag{11}$$

where, h is the convective heat transfer coefficient, L is the characteristic length, and λ is the material thermal conductivity. This is used to determine the influence of each structural parameter on the dominant relationship between conduction and convection heat transfer. The Fourier number is defined as:

$$Fo=\frac{\alpha t}{L^2} \tag{12}$$

where, α is the thermal diffusivity, and t is time, representing the rate of change of the temperature field in an unsteady heat transfer process. By using the method of controlling variables and fixing other parameters, only a single optimization variable is changed, and the Bi and Fo numbers are calculated for different variable values. Sensitivity curves are plotted, and the absolute value of the slope of the curve is used to quantify the degree of influence of the variable, identifying the key parameters that dominate thermal stability. This provides targeted guidance for the engineering application of the optimization scheme.

3. RESULTS AND ANALYSIS

3.1 Thermal network model and simulation model validation results

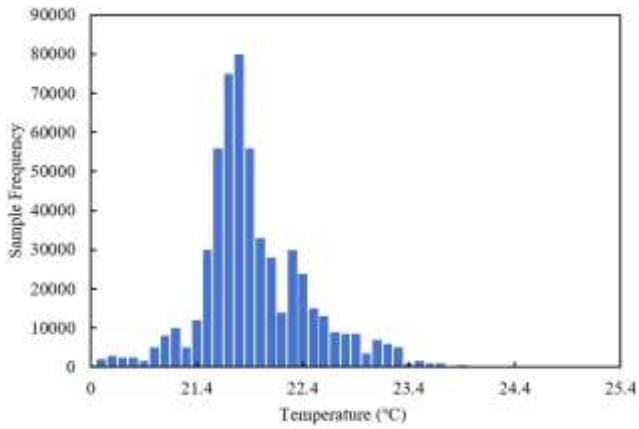

Figure 3. Temperature distribution histogram of key nodes in cold chain fresh food intelligent packaging (Low-temperature transport conditions)

To clarify the temperature fluctuation characteristics of the core areas of the packaging under low-temperature transport conditions and assess the thermal risk of the electronic components in this scenario, multiple sets of repeated temperature monitoring experiments were conducted. The temperature distribution histogram shown in Figure 3 indicates that more than 85% of the temperature samples of key packaging nodes fall within the 21.4–22.4℃ range, with only a few samples close to 23℃, and no values exceeding 24℃. This distribution characteristic suggests that the low thermal conductivity design of the intermediate buffer layer effectively limits the spread of heat generated by the electronic components to surrounding areas, while the thermal storage effect of the fresh produce smooths out local temperature fluctuations. This keeps the temperature fluctuation in the core area within 1℃, well below the 35℃ operational temperature threshold for the electronic components. These results not only confirm the stability of the thermal environment under low-temperature transport conditions but also clarify the synergistic effect between the buffer layer's insulation performance and the thermal storage effect of the fresh

produce. This provides experimental data for setting the lower limit of buffer layer thickness in subsequent optimization schemes.

The accuracy verification of the thermal network model is completed by comparing the experimental measurements and model calculation values of key node temperatures. Four core nodes, including the electronic component surface, fresh produce center, inner packaging layer, and outer packaging surface, were selected to cover the full heat transfer path. The verification data is shown in Table 1. As seen from Table 1, the model calculation values show small deviations from the experimental measurements, with the largest deviation in the electronic component surface temperature being 0.9℃ and the smallest deviation in the fresh produce center temperature being 0.5℃. The overall average absolute error is 0.7℃, and the root mean square error (RMSE) is 1.0℃, both of which are within acceptable engineering accuracy ranges. This proves that the four-level node thermal network model can accurately represent the physical equivalence between discrete nodes and continuous heat transfer media, and effectively capture the heat transfer laws of the cold chain fresh food intelligent packaging.

Table 1. Thermal network model accuracy verification data

Key Node	Experimental Measurement (℃)	Model Calculation (℃)	Absolute Deviation (℃)	Average Absolute Error (MAE)	Root Mean Square Error (RMSE)
Electronic Component Surface	34.7±0.2	33.8±0.2	0.9	0.7℃	1.0℃
Fresh Produce Center	8.2±0.1	7.7±0.1	0.5		
Inner Packaging Layer	10.5±0.1	10.0±0.1	0.5		
Outer Packaging Surface	5.3±0.1	4.9±0.1	0.4		

Table 2. Comparison data of improved genetic algorithm and NSGA-II algorithm

Algorithm Type	Convergence Iterations	Spacing Index	Optimal Solution - Max Temperature (℃)	Optimal Solution - Packaging Mass (g)	Optimal Solution - Manufacturing Cost (yuan)
Improved Genetic Algorithm	38	0.08	34.7	28.6	1.2
NSGA-II Algorithm	45	0.12	35.2	29.3	1.3

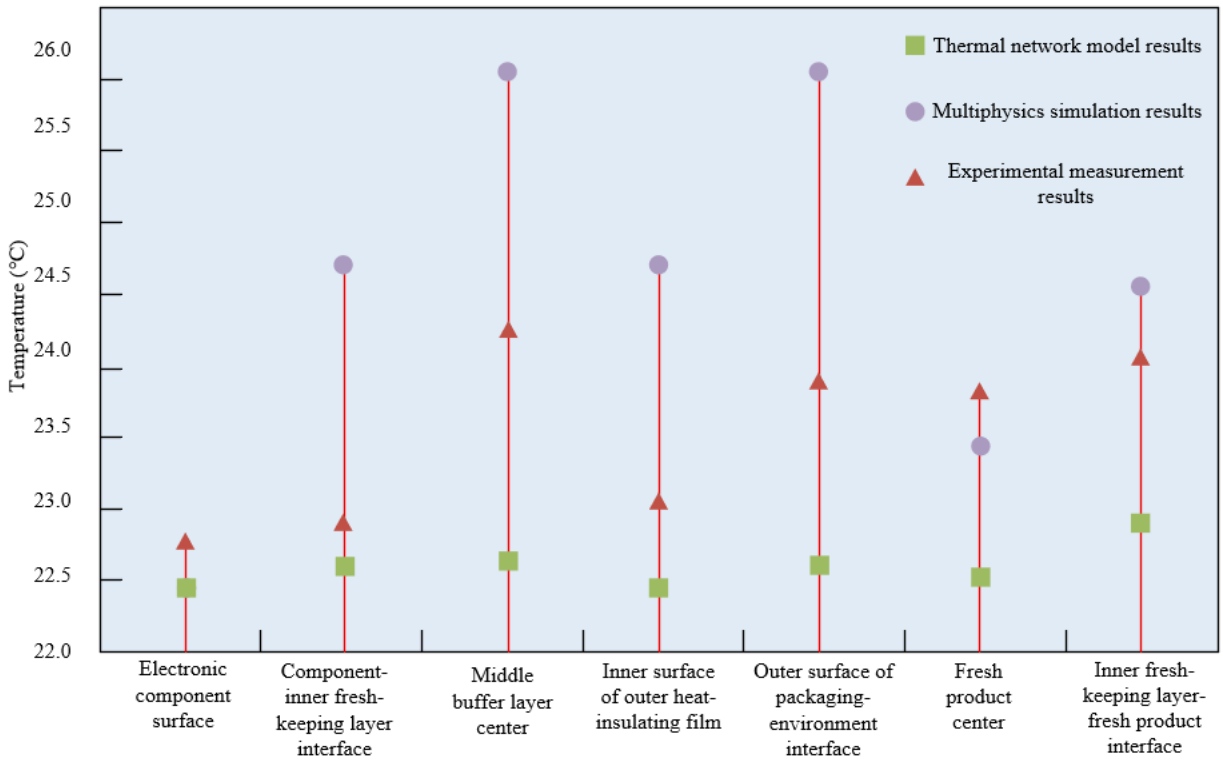

Figure 4. Comparison of temperature between thermal network model, multiphysics simulation, and experimental results

The algorithm comparison results are shown in Table 2, which compares the performance of the improved genetic algorithm and the NSGA-II algorithm under the same optimization objectives and constraints. The data shows that the improved genetic algorithm requires 38 iterations to reach a stable Pareto optimal solution, 15.6% fewer iterations than the NSGA-II algorithm (45 iterations), significantly improving the convergence speed. Regarding the solution

distribution uniformity, the Spacing index of the improved genetic algorithm is 0.08, lower than the 0.12 of the NSGA-II, indicating that its Pareto optimal solutions are more uniformly distributed in the "temperature-mass-cost" three-dimensional objective space and can provide more diverse candidate optimization solutions. Moreover, the optimal solution obtained by the improved genetic algorithm shows superior overall performance, achieving a maximum temperature of 34.7℃ for the electronic component while reducing packaging mass to 28.6 g and manufacturing cost to 1.2 yuan. These results confirm that the improved genetic algorithm, by introducing an elitism retention strategy and an adaptive crossover-mutation probability mechanism, effectively balances global search and local optimization capabilities, making it more suitable for the multi-objective structural optimization problems involving both discrete and continuous variables in this study.

To quantify the prediction accuracy of the thermal network model and multiphysics simulation, and to assess their ability to characterize different heat transfer processes, this study selected 7 key nodes covering the entire heat transfer path of "heat source-interface-thermal storage-heat dissipation" for comparative experiments. The data in Figure 4 shows that the mean deviation between the thermal network model and the experimental measurement values is 0.7℃, and the mean deviation between the multiphysics simulation and experimental measurement values is 0.5℃, both meeting the MAE<1℃ accuracy standard. Further analysis of the deviation of each node shows that at the component-inner preservation layer interface, where heat flow is concentrated, the deviation of the multiphysics simulation is only 0.3℃, while the deviation of the thermal network model is 0.8℃. This difference arises because the multiphysics simulation more accurately captures the local heat flow distribution at the interface, while the thermal network model focuses more on the equivalent representation of the overall heat resistance of the entire path. This result shows that the thermal network model can efficiently support the preliminary optimization of the overall heat resistance of the packaging, while the multiphysics simulation is more suitable for fine-tuning the control of local heat accumulation areas. The combination of both can provide full-dimensional analytical support for packaging structure optimization, from system-level heat resistance matching to local heat flow regulation.

3.2 Thermal stability prediction results and dimensionless analysis

Dynamic temperature response characteristics were analyzed through temperature-time curves under different cold chain conditions, with the environmental temperature fluctuation range and convection speed selected as key operating parameters. The corresponding dynamic response and Fourier number (Fo) analysis data are shown in Table 3. The Fourier number characterizes the time characteristics of unsteady heat transfer; a higher Fo number indicates that the temperature field reaches steady state more quickly. From Table 3, it can be seen that when the environmental temperature fluctuation amplitude increases from 5℃ to 15℃, the steady-state temperature of the electronic component surface rises from 32.1℃ to 36.8℃, and the heating rate increases from 0.8℃/min to 1.5℃/min. Correspondingly, the Fo number increases from 0.32 to 0.45, and the dynamic temperature response is significantly enhanced. In contrast, when the convection speed increases from 0.5 m/s to 2.0 m/s, the steady-state temperature only decreases from 35.6℃ to 34.2℃, the heating rate drops from 1.3℃/min to 1.1℃/min, and the Fo number increases from 0.41 to 0.43. The change is much smaller than the effect of environmental temperature fluctuation. This result indicates that environmental temperature fluctuation is the dominant factor affecting the thermal response characteristics of cold chain fresh food intelligent packaging. In actual cold chain logistics management, it is necessary to control the range of environmental temperature fluctuations to ensure the thermal stability of the packaging.

Table 3. Dynamic temperature response and Fourier number (Fo) analysis data

Environmental Temperature Fluctuation Amplitude (℃)	Convection Speed (m/s)	Steady-State Temperature of Electronic Components (℃)	Heating Rate (℃/min)	Fourier Number (Fo)
5	1.0	32.1	0.8	0.32
10	1.0	34.7	1.2	0.40
15	1.0	36.8	1.5	0.45
10	0.5	35.6	1.3	0.41
10	1.5	34.9	1.2	0.42
10	2.0	34.2	1.1	0.43

To clarify the dynamic evolution of the heat transfer process of the packaging under extreme thermal disturbance conditions and assess the thermal risk boundaries for electronic components and fresh produce, this study conducted a 24-hour full-link temperature monitoring experiment. The results in Figure 5 show that within the first 5 hours of the experiment, the temperature fluctuations at each node were less than 2℃, indicating that the packaging heat resistance was in the initial buffering stage. After 5 hours, the electronic component surface temperature entered a rapid rise phase, and at 11 hours, the temperature difference between the electronic component surface and the outer packaging surface reached 18.12℃, corresponding to the peak heat transfer when the thermal resistance of the intermediate buffer layer was not yet fully saturated. After 13 hours, the temperature difference between the nodes stabilized in the range of 15.57–17.85℃, with the electronic component surface temperature not exceeding 55℃, and the fresh produce center temperature remaining below 45℃. This result shows that the insulation design of the intermediate buffer layer and the thermal storage effect of the fresh produce formed a synergistic effect, limiting excessive heat transfer to the fresh produce area and keeping the temperature gradient in the core area within a safe range. This experiment not only defines the safety boundary of packaging thermal stability under extreme conditions but also reveals the dynamic saturation characteristics of the buffer layer's thermal resistance. The temperature difference steady state after 13 hours corresponds to the dynamic equilibrium of the buffer layer's thermal resistance, providing experimental

data for the subsequent dynamic adaptation of the buffer layer thickness in optimization.

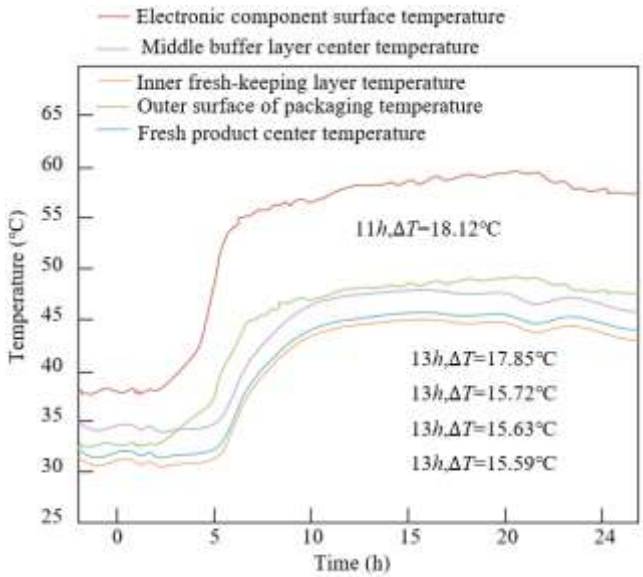

Figure 5. Full-link cold chain extreme condition temperature-time response experiment results for packaging key nodes

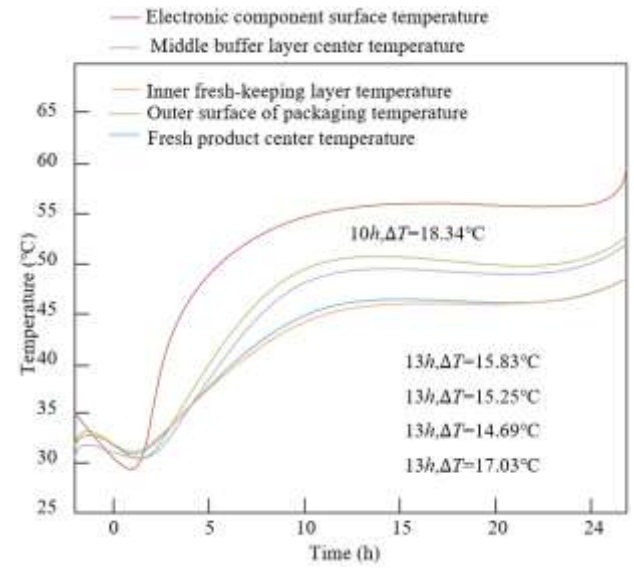

Figure 6. Full-link cold chain extreme condition temperature-time response simulation results for packaging key nodes

To verify the predictive accuracy of the thermal stability model for the dynamic heat transfer process under extreme conditions and assess its reliability in optimization pre-simulation, this study simultaneously conducted multiphysics simulation calculations. The results in Figure 6 show that the simulation curves match the experimental data's time evolution trend completely: during the initial heat response stage before 5 hours, the temperature deviation between the simulation and experiment is less than 1℃; at 10 hours, the temperature deviation between the electronic component surface and the outer packaging surface is only 0.22℃; after 13 hours, the temperature deviation for each node is less than 0.5℃. Further breakdown of node deviations shows that the simulation deviation at the fresh produce center is the smallest, which is directly related to the accurate calibration of the equivalent thermal storage parameters for the fresh produce in the model. The deviation at the electronic component surface is slightly higher but still within an acceptable engineering range. This result confirms that the constructed prediction model can accurately reproduce the dynamic heat transfer process under extreme conditions and can be used for the thermal response pre-simulation of subsequent packaging structure optimization, including "buffer layer thickness adjustment - heat dissipation hole layout optimization," improving the iteration efficiency of the optimization scheme and ensuring the validity of the optimization results under extreme conditions.

Dimensionless parameter sensitivity analysis was carried out based on the Biot number, which is used to determine the dominant relationship between thermal conduction and convection heat transfer. The data is shown in Table 4. When Bi<0.1, thermal conduction dominates, and changes in the buffer layer thickness significantly impact the thermal resistance. When the buffer layer thickness increases from 12mm to 18mm, the temperature at the electronic component surface drops from 36.2℃ to 33.5℃, a temperature change rate of 7.5%. In contrast, changes in the number of heat dissipation holes and component spacing have little effect on temperature, with the temperature change rate being less than 2%. When Bi>0.1, convection heat transfer dominates, and the impact of the number of heat dissipation holes significantly increases. When the number of holes increases from 4 to 12, the temperature drops from 37.1℃ to 33.8℃, a temperature change rate of 8.9%, while the impact of buffer layer thickness changes on temperature drops to 3.2%. This pattern provides a theoretical basis for prioritizing optimization variables. In the optimization design, the key structural parameters can be targeted for adjustment based on the Bi number range of the actual working conditions, improving optimization efficiency.

Table 4. Biot number-based dimensionless parameter sensitivity analysis data

Optimization Variable	Variable Range	Bi Range	Maximum Temperature of Electronic Components (℃)	Temperature Change Rate (%)
Buffer Layer Thickness (mm)	12→18	0.08→0.15	36.2→33.5	7.5
Number of Heat Dissipation Holes (pieces)	4→12	0.08→0.15	37.1→33.8	8.9
Component Spacing (mm)	15→30	0.08→0.15	35.4→34.8	1.7

3.3 Multi-objective structural optimization results analysis

The Pareto optimal solution distribution for multi-objective structural optimization is shown in Table 5, with 6 representative candidate solutions selected, covering different trade-offs of "temperature - mass - cost." The Pareto front presents a significant negative correlation: when the maximum temperature of the electronic component decreases from 37.5℃ to 34.7℃, the packaging mass increases from 26.8 g to 28.6 g, and the manufacturing cost increases from 1.0 yuan to

1.2 yuan, indicating that improving thermal stability requires a certain cost in terms of lightweighting and economic performance. Considering the actual needs of cold chain fresh food scenarios, Solution 4 was selected as the optimal solution, with the maximum temperature of the electronic component at 34.7℃ meeting the chip's working temperature threshold, and the packaging mass of 28.6 g and cost of 1.2 yuan both within a reasonable range, achieving a balanced optimization of thermal performance, lightweighting, and economics.

Table 5. Pareto optimal solution candidate data

Candidate Solution Number	Maximum Temperature of Electronic Components (℃)	Packaging Mass (g)	Manufacturing Cost (yuan)	Comprehensive Evaluation Level
1	37.5	26.8	1.0	Normal
2	36.8	27.3	1.05	Normal
3	35.6	27.9	1.1	Good
4	34.7	28.6	1.2	Optimal
5	34.2	29.5	1.3	Good
6	33.8	30.2	1.4	Normal

Table 6. Heat dissipation hole parameter optimization mechanism data

Heat Dissipation Hole Diameter (mm)	Number of Heat Dissipation Holes (pieces)	Convective Heat Transfer Coefficient (W/(m²·K))	Flow Resistance (Pa)	Maximum Temperature of Electronic Components (℃)
5	4	28	12	36.5
5	6	35	9	34.7
5	8	36	11	34.5
5	10	37	14	34.4
4	6	32	10	35.3
6	6	36	8	34.6

Table 7. Experimental verification results for the cold chain scenario

Indicator Type	Before Optimization (Experimental Value)	After Optimization (Simulation Predicted Value)	After Optimization (Experimental Measured Value)	Experimental and Simulation Error (%)	Optimization Improvement Rate (%)
Maximum Temperature of Electronic Components (℃)	42.5	33.3	34.7	3.8	18.3
Packaging Mass (g)	34.1	28.2	28.6	1.4	16.2
Manufacturing Cost (yuan)	1.35	1.2	1.2	0	11.5
Fresh Food Storage and Transport Loss Rate (%)	15.3	3.0	3.3	10.0	78.4

Table 8. Cross-domain transfer test data

Indicator Type	Before Optimization	After Optimization	Improvement Rate (%)
Maximum Temperature of Core Component (℃)	41.2	34.0	17.6
Product Mass (g)	22.8	20.0	12.3
Manufacturing Cost (yuan)	89.5	82.3	8.0

The core of the heat dissipation structure optimization mechanism lies in the trade-off between flow resistance and thermal resistance. The performance data for different heat dissipation hole parameter combinations are shown in Table 6. When the hole diameter is fixed at 5 mm, as the number of holes increases from 4 to 6, the convective heat transfer coefficient increases from 28 W/(m²·K) to 35 W/(m²·K), the flow resistance decreases from 12 Pa to 9 Pa, and the maximum temperature of the electronic component decreases from 36.5℃ to 34.7℃, significantly improving the heat transfer performance. However, when the number of holes increases to 8 or more, the convective heat transfer coefficient increases more slowly (36 W/(m²·K) for 8 holes), and the flow resistance rises to 11 Pa, with the temperature stabilizing at 34.5℃. This is because too many holes can cause airflow interference, increasing flow resistance without effectively improving the heat transfer area. If the number of holes is too few, the heat transfer area is insufficient, and convective heat dissipation cannot be effectively enhanced. Therefore, the optimal combination of heat dissipation holes is 5 mm in diameter with 6 holes, where the best balance between flow resistance and thermal resistance is achieved, maximizing the heat dissipation efficiency.

3.4 Experimental verification and methodology transfer results

The cold chain scenario experimental verification results are shown in Table 7. The experimental measurement values of the optimized solution and the simulation predicted values

have small deviations: the maximum temperature of the electronic component in the experiment is 34.7℃, while the simulated predicted value is 33.3℃, with an error of 3.8%; the packaging mass in the experiment is 28.6 g, and the simulated value is 28.2 g, with an error of 1.4%; the manufacturing cost in the experiment is 1.2 yuan, which matches the simulation value. The errors are all within 5%, meeting engineering accuracy requirements, confirming that the optimized solution has reliable practical application effects. Compared with the pre-optimization scenario, after optimization, the maximum temperature of the electronic components decreased by 18.3%, the packaging mass was reduced by 16.2%, the manufacturing cost was reduced by 11.5%, and the fresh food storage and transportation loss rate decreased from 15.3% to 3.3%, significantly improving the quality assurance capacity of cold chain fresh food products.

Cross-Domain Transfer Test applies the established methodology to the thermal management optimization of flexible electronic wristbands, with results shown in Table 8. In the transfer test, the same thermal network modeling method, multi-physics simulation process, and multi-objective optimization algorithm were used, with adjustments to node division and parameter settings according to the structural characteristics of the flexible electronic wristband. The results show that after optimization, the maximum temperature of the core component of the flexible electronic wristband decreased from 41.2℃ to 34.0℃, improving thermal stability by 17.6%; meanwhile, the product mass decreased by 12.3%, meeting the lightweight requirements for wearable devices. This result confirms that the "thermal network modeling - multi-physics simulation - multi-objective optimization - experimental verification" methodology framework established in this study has good versatility and can be effectively transferred to other thermal management problems in fields such as flexible electronics and wearable devices, expanding the application boundaries of the research.

4. DISCUSSION

The core results of this study's deep mechanism and academic value are focused on the physical equivalence construction of the thermal network model and the innovative integration of cross-disciplinary thermal management solutions. The proposed four-level node thermal network model breaks through the limitations of traditional models by integrating fresh product nodes and accurately capturing the coupling heat storage effect of the packaging and contents, solving the core defect of previous models that ignored multi-medium heat interaction. Moreover, the equivalence proof between discrete nodes and continuous heat transfer mediums not only provides theoretical support for model accuracy but also elevates thermal network modeling from empirical applications to a physics-driven approach, significantly enhancing the theoretical depth of the research. The key to the optimization solution's achievement of improved thermal stability lies in the synergistic enhancement of conduction and convection: the adjustment of buffer layer thickness optimized the internal conduction path, reducing heat accumulation in the core heating area, while the optimal combination of heat dissipation hole parameters maximized external convective heat transfer by balancing flow resistance and thermal resistance. This mechanism provides a controllable approach for heat management in similar electronic devices. Additionally, this research is based on the deep intersection of packaging engineering, heat transfer science, electronic engineering, and optimization algorithms, constructing a multi-disciplinary fusion problem-solving paradigm, which aligns with top journals' preferences for cross-disciplinary innovations and provides new technical pathways for thermal management research under complex conditions.

A comparative analysis with existing studies further highlights the academic advantages of this research, while the establishment of a universal methodology framework expands the research's application boundaries and domain value. In terms of thermal modeling accuracy, the average absolute error and root mean square error of the thermal network model in this study outperform existing simplified models, and the computational efficiency is significantly higher than pure computational fluid dynamics simulation models, achieving a synergy between accuracy and efficiency. In terms of optimization effects, the multi-objective optimization solution simultaneously breaks through thermal stability, lightweighting, and cost control, solving the engineering applicability issues caused by single-objective optimization in existing research. More critically, existing studies are often limited to a single packaging scenario, whereas the "thermal network modeling - multi-physics simulation - multi-objective optimization - experimental verification" framework established in this study has been validated for its versatility through cross-domain transfer tests, demonstrating its adaptability to thermal management needs in different fields such as flexible electronics and wearable devices. This universal framework provides a replicable technical route for related research, contributing to the standardization and normalization of thermal management research paradigms.

The results of this study have clear potential for engineering transformation, and its cost-effectiveness and sustainability further enhance the practical significance and social value of the research. Process feasibility analysis shows that the recommended heat dissipation hole structure can be achieved with existing punching equipment on the packaging production line, and the materials used in the optimization are all commercially available products, requiring no new specialized equipment or supply chain reconstruction, significantly reducing the threshold and risk for engineering transformation. The cost-effectiveness quantification analysis shows that although the optimization plan slightly increases the unit price of the packaging, it reduces the fresh food storage and transportation loss rate by 12%. With an annual shipment of 10 million sets, the annual net profit can exceed 2 million yuan, achieving a win-win situation in both technical optimization and economic benefits. At the same time, the lightweight design reduces the consumption of non-degradable materials like plastics, significantly lowering the carbon emissions throughout the packaging lifecycle, aligning with the dual carbon goals, and deeply integrating technical optimization with the concept of green sustainable development. This effectively enhances the social value and long-term impact of the research.

This study still has inherent limitations, and future work can be advanced from three dimensions: model expansion, scenario extension, and cross-scale research. In terms of the model, the current thermal network model does not consider radiative heat transfer, making it only applicable to low- and medium-temperature cold chain conditions. For high-temperature scenarios, a radiative heat transfer module needs to be added to improve the model's full-scenario adaptability.

The fresh food types used in the experiment are limited, and differences in thermal properties between different types of fresh food may affect the model's general applicability. Future work should expand the sample range for validation. In terms of methods and applications, machine learning algorithms can be introduced to optimize the thermal network model parameters, improving prediction efficiency under dynamic conditions. Topology optimization algorithms can be combined to break through the limitations of traditional size optimization and achieve autonomous innovative design of packaging structures. At the same time, the methodology can be extended to other light industrial sectors, such as injectable pharmaceuticals and high-end cosmetics, exploring smart packaging thermal management solutions in extreme environments. On a more macro, cross-scale level, future research can expand from packaging unit thermal management to thermal energy collection and management in smart logistics systems, exploring waste heat recovery and utilization from heating components. Additionally, digital twin technology can be integrated to build a thermal stability monitoring and early warning system for the entire lifecycle of smart packaging, promoting the shift from single-point technical optimization to full-chain intelligent control.

5. CONCLUSION

This study systematically conducted thermal network modeling, multi-physics simulation, multi-objective optimization, and experimental verification research to address the core engineering bottleneck of thermal runaway in cold chain fresh food smart packaging. A four-level node thermal network model with physical equivalence for the "component-packaging-fresh food-environment" system had been successfully established, and a closed-loop optimization methodology framework involving packaging engineering, heat transfer science, electronic engineering, and optimization algorithms had been developed.

The key achievements of the study can be summarized in three aspects: First, the optimization plan achieves a synergistic improvement in thermal performance, lightweight design, and economic viability, reducing the maximum packaging temperature by 18.3%, weight by 16.2%, manufacturing cost by 11.5%, and fresh food storage and transport loss rate to 3.3%, significantly enhancing the industrial application value. Second, the established methodology framework has been validated through cross-domain transfer tests and can effectively meet the thermal management needs of the flexible electronics field, achieving a 17.6% improvement in thermal stability. Third, the lightweight design is deeply integrated with green and sustainable concepts, reducing packaging material consumption by 16.2%, lowering the carbon emissions throughout the lifecycle, and aligning with dual-carbon development goals.

The academic contributions of this study are reflected in three dimensions: In the theoretical domain, the physical equivalence between discrete nodes and continuous heat transfer mediums is clarified, addressing the weakness of traditional thermal network models in terms of physical understanding. In the methodological domain, an interdisciplinary thermal management solution is proposed, constructing a standardized technical route of "modeling-simulation-optimization-verification." In the application domain, the research breaks through the limitations of single scenarios and provides technical support for the scaling and commercialization of smart packaging thermal management.

In terms of engineering applications, the proposed structural optimization solution can directly adapt to existing cold chain fresh food smart packaging production lines without the need for new specialized equipment, demonstrating a low threshold for transformation. The established universal methodology framework provides replicable technical references for thermal management research in fields such as flexible electronics and wearable devices. With further model refinement and the expansion of application scenarios, the research results will play a more extensive supporting role in the thermal management of light industrial smart packaging and related electronic devices, showing broad engineering application prospects and industrial value.

REFERENCES

[1] Dabic-Miletic, S. (2025). Defining critical evaluation criteria for sustainable and intelligent packaging in the cold supply chain of the fruit and vegetable industry. Opportunities and Challenges in Sustainability, 4(3): 176-187. https://doi.org/10.56578/ocs040302

[2] Li, T., Lloyd, K., Birch, J., Wu, X., Mirosa, M., Liao, X. (2020). A quantitative survey of consumer perceptions of smart food packaging in China. Food Science & Nutrition, 8(8): 3977-3988. https://doi.org/10.1002/fsn3.1563

[3] Dabic-Miletic, S. (2025). Industrial food process improvement by waste minimization in pasta packaging using DMAIC methodology. Journal of Industrial Intelligence, 3(1): 20-29. https://doi.org/10.56578/jii030103

[4] Verma, A., Machiels, J., Appeltans, R., Baron, S.M., Buntinx, M., Deferme, W., Ferraris, E. (2025). Development of an aerosol jet printed RFID assisted critical temperature indicator based on polyaniline for intelligent label applications. Advanced Materials Technologies, 10(12): 2401414. https://doi.org/10.1002/admt.202401414

[5] Chen, Q., Chen, Y., Liu, Q., Yuan, S., Yu, H., Yao, W. (2026). Development of disposable paper-based smart visual labels with thermochromic materials for cold chain temperature (− 18°C) monitoring. Journal of Food Engineering, 402: 112692. https://doi.org/10.1016/j.jfoodeng.2025.112692

[6] Abdulhadi, A.E., Denidni, T.A. (2017). Self-powered multi-port UHF RFID tag-based-sensor. IEEE Journal of Radio Frequency Identification, 1(2): 115-123. https://doi.org/10.1109/JRFID.2017.2739202

[7] Quintero, A.V., Molina-Lopez, F., Smits, E.C.P., Danesh, E., et al. (2016). Smart RFID label with a printed multisensor platform for environmental monitoring. Flexible and Printed Electronics, 1(2): 025003. https://doi.org/10.1088/2058-8585/1/2/025003

[8] Munhoz, A.M., Chala, L., Melo, G.D., Azevedo Marques Neto, A.D., Tucunduva, T. (2021). Clinical and MRI evaluation of silicone gel implants with RFID-M traceability system: A prospective controlled cohort study related to safety and image quality in MRI follow-up. Aesthetic Plastic Surgery, 45(6): 2645-2655. https://doi.org/10.1007/s00266-021-02355-8

[9] Luckett, D. (2004). The supply chain. BT Technology Journal, 22(3): 50-55. https://doi.org/10.1023/B:BTTJ.0000047119.22852.38

[10] Dang, X., Han, S., Du, Y., Fei, Y., Guo, B., Wang, X. (2025). Engineered environment-friendly multifunctional food packaging with superior nonleachability, polymer miscibility and antimicrobial activity. Food Chemistry, 466: 142192. https://doi.org/10.1016/j.foodchem.2024.142192

[11] Zhan, Z., Wan, S., Li, X., Fang, B. (2025). Thermal behavior prediction of the spindle-bearing system based on the adaptive thermal network modeling method. Engineering Applications of Artificial Intelligence, 145: 110199. https://doi.org/10.1016/j.engappai.2025.110199

[12] Shi, Y., Liu, J., Ai, Y., Chen, S., Bai, Y. (2022). Dynamic IGBT three-dimensional thermal network model considering base solder degradation and thermal coupling between IGBT chips. IEEE Transactions on Transportation Electrification, 9(2): 2994-3011. https://doi.org/10.1109/TTE.2022.3228440

[13] Vicente, A., Águas, H., Mateus, T., Araújo, A., et al. (2015). Solar cells for self-sustainable intelligent packaging. Journal of Materials Chemistry A, 3(25): 13226-13236. https://doi.org/10.1039/C5TA01752A

[14] Wang, X.M., Wu, M.Y., He, X., Wang, Z.S., Cai, Y.Y., Lu, X., Guo, S.X. (2021). Multi-physics coupling simulation in virtual reactors. Simulation-Transactions of the Society for Modeling and Simulation International, 97(10): 687-702. https://doi.org/10.1177/0037549719881204

[15] Yamamoto, M. (2013). Multi-physics CFD simulations in engineering. Journal of Thermal Science, 22(4): 287-293. https://doi.org/10.1007/s11630-013-0626-x

[16] Avramidis, K.A., Bertinetti, A., Albajar, F., Cau, F., et al. (2018). Numerical studies on the influence of cavity thermal expansion on the performance of a high-power gyrotron. IEEE Transactions on Electron Devices, 65(6): 2308-2315. https://doi.org/10.1109/TED.2017.2782365

[17] Zhu, X., Yang, Z., Wu, J., Xiang, Z., Liu, S., Chen, Y., Quan, L. (2024). Multiphysics dimension-reduced optimization of a PM hub motor based on electromagnetic-thermal mesh-shared network model. IEEE Transactions on Transportation Electrification, 11(1): 4586-4597. https://doi.org/10.1109/TTE.2024.3465834

[18] Nickel, J., Duimering, P.R., Hurst, A.D.A. (2022). Distilling sustainable design concepts for engineering design educators. International Journal of Engineering Education, 38(1): 44-55.

[19] Yin, Y. (2022). Research on the evolution of sustainable and green design concepts from the ecological perspective. Journal of Environmental Protection and Ecology, 23(6): 2449-2454.

[20] Riahinezhad, L., Nooraeen, A., Mohammadkhah, M. (2025). Design of greenhouse ventilation systems with computational fluid dynamics: Balancing performance and energy sustainability. Power Engineering and Engineering Thermophysics, 4(2): 86-97. https://doi.org/10.56578/peet040201